Tuning Edge States in Strained-Layer InAs/GaInSb Quantum Spin Hall Insulators

Lingjie Du,[1] Tingxin Li,[1,2] Wenkai Lou,[3] Xingjun Wu,[2] Xiaoxue Liu,[2] Zhongdong Han,[2]
Chi Zhang,[2,4] Gerard Sullivan,[5] Amal Ikhlassi,[5] Kai Chang,[3] and Rui-Rui Du[1,2,4,*]

[1]*Department of Physics and Astronomy, Rice University, Houston, Texas 77251-1892, USA*
[2]*International Center for Quantum Materials, School of Physics, Peking University, Beijing 100871, China*
[3]*SKLSM, Institute of Semiconductors, Chinese Academy of Sciences, Beijing 100083, China*
[4]*Collaborative Innovation Center of Quantum Matter, Beijing 100871, China*
[5]*Teledyne Scientific and Imaging, Thousand Oaks, California 91603, USA*
(Received 9 October 2016; published 3 August 2017)

We report on a class of quantum spin Hall insulators (QSHIs) in strained-layer InAs/GaInSb quantum wells, in which the bulk gaps are enhanced up to fivefold as compared to the binary InAs/GaSb QSHI. Remarkably, with consequently increasing edge velocity, the edge conductance at zero and applied magnetic fields manifests time reversal symmetry-protected properties consistent with the Z_2 topological insulator. The InAs/GaInSb bilayers offer a much sought-after platform for future studies and applications of the QSHI.

Introduction.—The time reversal symmetry (TRS) protected quantum spin Hall effect (QSHE) is predicted in a two-dimensional topological insulator [1–4] with a topological number Z_2. The transport evidence for the QSHE was first observed [5] in a HgTe/CdTe quantum well (QW) with its edge conductance quantized to the theoretical value. To date the leading material systems are made of semiconductor QWs, i.e., HgTe/CdTe QW and inverted InAs/GaSb QWs; both are described by the Bernevig-Hughes-Zhang model [4]. In InAs/GaSb QWs, wavefunction hybridization between InAs and GaSb layers dominates the bulk and opens a minigap Δ [6], while a Kramer's pair of spin-momentum-locked edge states emerges on the device perimeters [7]. Relevant experiments are reported in Refs. [8–17]. The charge transport in helical edges is dissipationless, owing to the notion that the helical property prevents charge backscattering. On the other hand, theories [18–20] taking into account electron-electron interactions and correlations suggest that certain many-body scattering processes may exist, which should lead to dissipation.

In the inverted InAs/GaSb bilayer system, the ground electron sub-band in the InAs well and the ground hole sub-band in the GaSb well cross at certain wave vectors k_{cross}. Spatially separated electrons and holes are strongly coupled at this crossing point due to the tunneling between the two wells; consequently, a hybridization gap Δ is opened at k_{cross}, which is the bulk gap of the quantum spin Hall insulator (QSHI). The density of the charge neutral point (CNP) in the inverted regime is referred to as $n_{\mathrm{cross}} = k_{\mathrm{cross}}^2/2\pi$. The degree of band inversion can be tuned by QW widths and gate voltages [6,8–16], and it has dramatic influences on the bulk transport properties. In the deeply inverted regime where typically n_{cross} above $\sim 2 \times 10^{11}$ cm^{-2}, there always exist

considerable residual states in the hybridization gap; thus, the bulk of InAs/GaSb QWs is not truly insulating [8,9,12,13], which limits the studies and applications of the QSHE.

On the other hand, in the shallowly inverted regime (n_{cross} below $\sim 1 \times 10^{11}$ cm^{-2}), the bulk is insulating to a high degree and quantized helical edge conductance plateaus were observed [10,15]. Surprisingly, the quantized conductance plateaus persist under external magnetic fields, in contrast with the theoretical expectations for TRS protected helical edge states [10]. On a general ground, Coulomb interactions of electron-hole pairs dominate over hybridization effects in such a dilute limit [21], leading to the possibility of a two-dimensional excitonic ground state [21–23]. Moreover, here the edge Fermi velocity $v_F \sim \Delta/2\hbar k_{\mathrm{cross}}$ is unusually small, in the range of $\sim 2 \times 10^4$ ms^{-1} to $\sim 5 \times 10^4$ ms^{-1}, indicating that the edge states are in a strongly interacting regime [18,20,24]. Overall, while the quantized edge transport has been observed in micrometer-size samples of shallowly inverted InAs/GaSb, the resilience to external magnetic field and the observed length dependence in long samples are not accounted for by the single-particle model. From an experimental perspective, it is much more desirable to develop a plain vanilla QSHI with properties dominated by single-particle physics. Ideally, to some degree the interaction effects may be set in by tuning experimental parameters such as v_F.

In this Letter, we report on a QSHI in strained-layer InAs/GaInSb QWs, which clearly manifests TRS protected properties. Because of the band structural changes from the strain effect, QWs can be made narrower, leading to stronger overlaps between electron and hole wave functions. This effect results in insulating hybridization gaps at low temperatures even when the n_{cross} is larger than

3×10^{11} cm^{-2}. In addition, the helical edge conductance decreases under either perpendicular or in-plane magnetic fields, indicating the opening of mass gaps in the edge states. Remarkably, we found that the edge conductance and the magnetic response are correlated with v_F, which could be well controlled by lattice strain and the gate voltages.

Strain effect in InAs/GaInSb.—Strain engineering is a common way to modify the band structure and physical properties for semiconductor materials, and recently for topological materials [25,26]. Specific to the InAs/GaInSb system, the strained-layer InAs/Ga$_{1-x}$In$_x$Sb superlattice (SL) infrared detectors were proposed [27] by Smith and Maihiot in 1987. By alloying GaSb (the lattice constant about 6.1 Å) with InSb (6.4 Å), because of the strain in the growth plane, the energy of the conduction band (CB) in InAs shifts downward while the energy level of the valence band (VB) in GaInSb splits into the heavy hole (HH) level and light hole (LL) level, respectively, where the energy of the HH level is higher than the original top VB in GaSb. As a result, to reach a fixed energy band gap, the layers of the InAs/GaInSb SL are made narrower than the InAs/GaSb SL, thereby increasing the optical absorption efficiency. Such strain engineering has led to the invention of high-performance long-wavelength SL infrared detectors [28].

A similar physics idea may guide the construction of a large-gap QSHI. Based on the strain effects described above, we can reach the same inverted band structure with narrower QWs in strained-layer InAs/GaInSb, comparing to unstrained InAs/GaSb. The hybridization-induced gap should increase in such narrower QWs primarily due to the enhanced overlap of electron and hole wave functions. In addition, due to the energy splitting of the HH and LH in GaInSb, the Fermi surface of electrons would better match with the Fermi surface of holes, which also help to reduce the residual nonhybridized carriers.

Figures 1(a)–1(c) show calculated band structure of strained InAs/Ga$_{1-x}$In$_x$Sb QWs with different indium concentrations ($x = 0.20, 0.25, 0.32$) by the eight-band Kane model. The results indicate that a ~20 meV hybridization gap could be attained in the [100] direction in InAs/Ga$_{0.68}$In$_{0.32}$Sb QWs, which is about a fivefold enhancement from the value ~4 meV in unstrained InAs/GaSb QWs. Depending on gating conditions, the measured bulk gap is around this value. The wafers we used for the present experiment were grown by molecular beam epitaxy (MBE). As an example, the structure of a 9.5 nm InAs/4 nm Ga$_{0.75}$In$_{0.25}$Sb QWs is shown in Fig. 1(e). Figure 1(f) is a transmission electron microscope (TEM) photograph of an InAs/Ga$_{0.68}$In$_{0.32}$Sb wafer; it shows that the crystalline structure remains coherent across the heterostructure interfaces regardless of ~1.5% in-plane strain.

Transport properties of bulk states in strained-layer InAs/GaInSb QWs.—In order to directly measure the bulk conductance, we fabricate dual-gated Corbino devices.
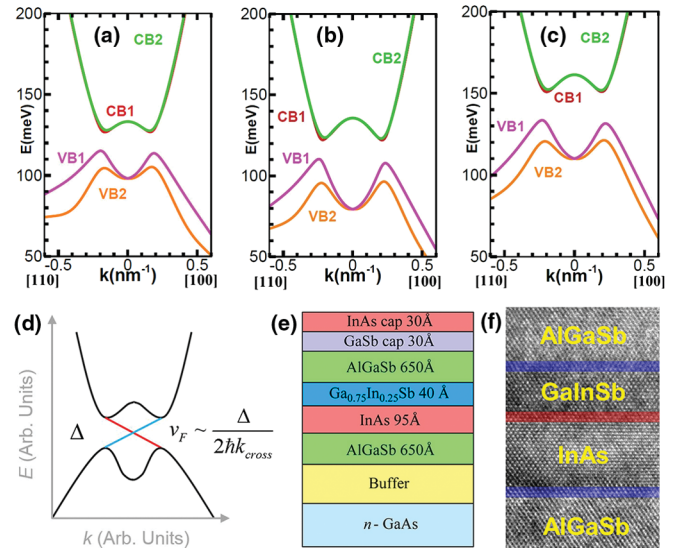

FIG. 1. Calculated band dispersions and wafer structures of the strained InAs/GaInSb QWs. [(a)–(c)] Calculated bulk band structure of the InAs/Ga$_{0.80}$In$_{0.20}$Sb (8.7/4 nm) QWs, InAs/Ga$_{0.75}$In$_{0.25}$Sb (9/4 nm) QWs, and InAs/Ga$_{0.68}$In$_{0.32}$Sb (8/4 nm) QWs; CB1, VB1 and CB2, VB2 are bands of different spin component. (d) Schematic drawing of band dispersion (both bulk states and edge states) in the InAs/GaInSb QSHI system. (e) Wafer structures of the strained-layer InAs/Ga$_{0.75}$In$_{0.25}$Sb QWs used for experiments. (f) Shown here as an example, a TEM photograph of the strained InAs/Ga$_{0.68}$In$_{0.32}$Sb wafer; blue and red lines are a guide for the eyes.

In this case, the edge conductance is shunted and has no contribution to the signals. Figures 2(a), 2(c) and 2(b), 2(d) show the traces of the conductivity versus front-gate voltage V_{front} measured from a Corbino device made by the InAs/Ga$_{0.75}$In$_{0.25}$Sb QWs at temperature $T \sim 20$ mK, with back gate voltage $V_{\text{back}} = 0$ V and $V_{\text{back}} = 4$ V, respectively. At the CNP, the conductivity show dips, indicating the entrance into an energy gap. For more positive V_{back}, the bulk band becomes more inverted, resulting in a less insulating bulk. Nevertheless, the bulk conductivity is still negligible at low temperature, about 100 MΩ per square at 20 mK for the $V_{\text{back}} = 0$ V case, and about 25 MΩ per square at 20 mK for the $V_{\text{back}} = 4$ V case. Note that even for the $V_{\text{back}} = 0$ V case, the n_{cross} value of this wafer is larger than 2×10^{11} cm^{-2}, corresponding to the modestly deep-inverted regime. Hybridization gaps with residual conductivity have been commonly reported in deeply inverted InAs/GaSb QWs [6,8,12,13]; this is the first time that a substantially insulating hybridization gap is observed at low temperature.

Electron-hole hybridization is most favored when the Fermi momentum of electrons k_F^e and holes k_F^h is equal. Under in-plane magnetic field $B_{//}$, applied along the x axis of the example, Lorenz force gives tunneling carriers additional momentum along the y axis, resulting in a relative shift of band dispersions $\Delta k_y = -eB\Delta\langle z \rangle / h$
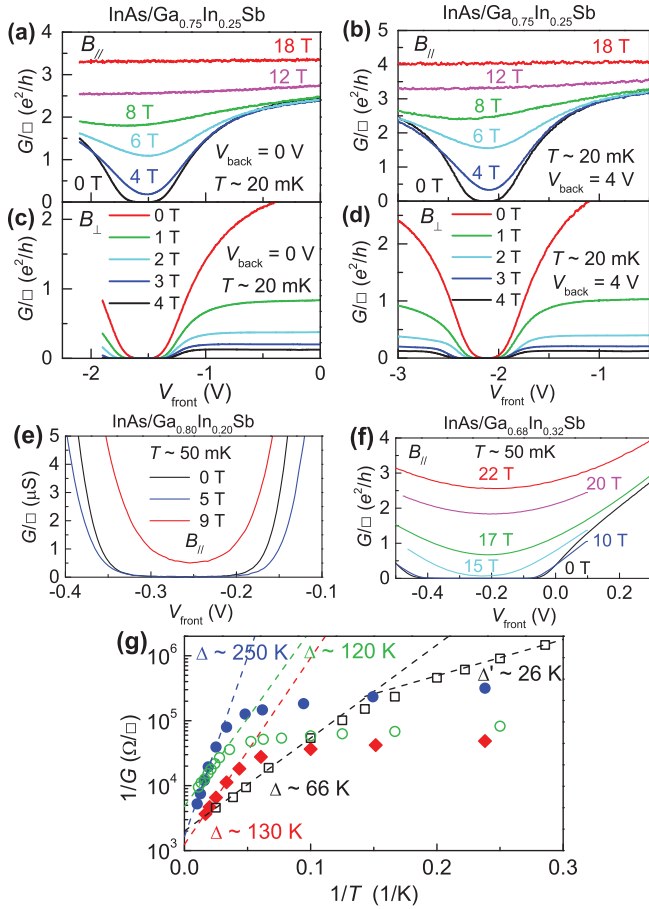
FIG. 2. Transport data of bulk states from Corbino devices. G-V_{front} traces of a InAs/Ga$_{0.75}$In$_{0.25}$Sb Corbino under different in-plane magnetic field at (a) $V_{\text{back}} = 0$ V and (b) $V_{\text{back}} = 4$ V. G-V_{front} traces under different perpendicular magnetic fields at (c) $V_{\text{back}} = 0$ V and (d) $V_{\text{back}} = 4$ V. G-V_{front} traces under different in-plane magnetic fields for (e) a InAs/Ga$_{0.80}$In$_{0.20}$Sb Corbino and (f) a InAs/Ga$_{0.68}$In$_{0.32}$Sb Corbino. (g) Arrhenius plots for InAs/GaSb QWs (open squares), InAs/Ga$_{0.80}$In$_{0.20}$Sb QWs (open circles), InAs/Ga$_{0.75}$In$_{0.25}$Sb QWs (filled diamonds), and InAs/Ga$_{0.68}$In$_{0.32}$Sb QWs (filled circles). Energy gaps are deduced by fitting $G_{xx} \propto \exp(-\Delta/2k_B T)$, as shown by straight dash lines in the plot. Here k_B is the Boltzmann constant.

(tunneling distance $\Delta\langle z \rangle$ is limited by one-half thickness of the QWs). Consequently, carrier hybridization is suppressed due to momentum mismatch, rendering the QWs as a bilayer semimetal. As shown in Figs. 2(a) and 2(b), the gap at the CNP is gradually closed with an increasing $B_{//}$. Similar behaviors have also been observed in the InAs/Ga$_{0.80}$In$_{0.20}$Sb QWs [Fig. 2(e)] and InAs/Ga$_{0.68}$In$_{0.32}$Sb QWs [Fig 2(f)]. This observation agrees with the behavior of a hybridization gap under the in-plane magnetic field, but in contrast to the behavior of the insulating gap observed in a shallowly inverted InAs/GaSb QW [23], where the bulk gap does not show sign of closing in a very high field. Under perpendicular magnetic
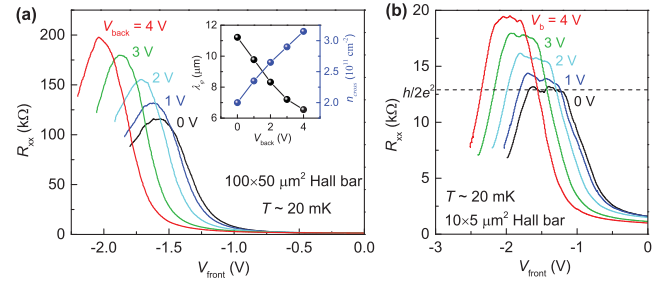

FIG. 3. Helical edge transport in strained-layer InAs/Ga$_{0.75}$In$_{0.25}$Sb QWs. R_{xx}-V_{front} traces measured from (a) a 100×50 μm Hall bar device and (b) a 10×5 μm Hall bar device at $T \sim 20$ mK with $V_{\text{back}} = 0, 1, 2, 3,$ and 4 V. The edge characteristic length increases with decreasing V_{back}. The inset in (a) shows the λ_φ and the n_{cross} values at different back-gate bias V_{back}.

field $B_\perp$, the bulk becomes more insulating due to localization effects, as shown in Figs. 2(c) and 2(d).

Information of the bulk gaps can be further obtained from temperature dependent conductance. Figure 2(g) shows the Arrhenius plots of Corbino devices made of strained-layer InAs/Ga$_{1-x}$In$_x$Sb QWs ($x = 0.20, 0.25,$ and 0.32) and the shallowly inverted InAs/GaSb QWs (data adapted from Ref. [10] at $B = 0$ T). It lacks the exponential dependences in the tail regime for the strained-layer wafers; the transport there is more like variable-range hopping. Indeed, this is a characteristic feature for transport in the hybridization gap, as discussed in Ref. [8]. At higher temperatures, the hybridization gap values can be estimated by fitting the Arrhenius plots, which is ~ 66 K for the shallowly inverted InAs/GaSb QWs, ~ 120 K for the InAs/Ga$_{0.80}$In$_{0.20}$Sb QWs, ~ 130 K for the InAs/Ga$_{0.75}$In$_{0.25}$Sb QWs, and ~ 250 K for the InAs/Ga$_{0.68}$In$_{0.32}$Sb QWs. Overall, larger hybridization gaps have been achieved by strain engineering, in reasonable agreement with the calculations.

Controllable helical edge states with long characteristic length.—We now turn to the helical edge properties of strained-layer InAs/Ga$_{0.75}$In$_{0.25}$Sb QWs. Figure 3(a) shows the longitudinal resistance R_{xx}-V_{front} traces of a 100×50 μm Hall bar device with various V_{back} at $T \sim 20$ mK. Here the measured R_{xx} solely results from the edge channels, since the bulk is fully insulating at such low T. At $V_{\text{back}} = 0$ V, the resistance peak is about 115 kΩ, corresponding to a characteristic length λ_φ (which refers to a length scale at which dissipationless edge transport breaks down and counterpropagating spin-up and spin-down channels equilibrate) of about 11 μm. The λ_φ of different devices made by this wafer typically range from ~ 5 to 10 μm, significantly longer than those in previous studies [5,10] of the QSHI. Moreover, the λ_φ can be tuned by gate: as shown in Fig. 3(a) the resistance peak values gradually decrease with decreasing V_{back} (namely, less inverted), indicating that the λ_φ increase from ~ 6 μm at $V_{\text{back}} = 4$ V to ~ 11 μm at $V_{\text{back}} = 0$ V. (Note that for this device the back-gate bias

was limited within 4 and 0 V). The insets of Fig. 3(a) illustrate the λ_φ and the n_{cross} (deduced from magnetotransport data) versus V_{back}.

According to the definition of characteristic length, if the device edge length is shorter than λ_φ, the edge conductance measured should be quantized to $2e^2/h$. This is indeed confirmed in a Hall bar device of length 10 μm, as shown in Fig. 3(b). As the λ_φ is being tuned from 6 to 11 μm, the R_{xx} decreases, and finally reaches a plateau of 12.9 kΩ with a reasonable accuracy.

A plausible explanation for the above data is related to the interaction effects [18–20] in the helical edge state. At more positive V_{back}, the bulk band becomes more inverted, and hence a larger k_{cross} and a roughly constant Δ [7]; overall this leads to a smaller Fermi velocity $v_F \sim \Delta/2\hbar k_{cross}$ of the helical edge states, resulting in more prominent interaction effects for the edge states. The backscattering processes enhance when the electron-electron interactions become stronger; thus, the helical edge states exhibit a shorter characteristic length in the more inverted case.

TRS-protected helical edge states.—In general, applying the magnetic field breaks the TRS and opens a gap in the helical edge states. The one-dimensional massless Dirac fermion could be tuned into a one-dimensional massive fermion allowing for backscattering; thereby the helical edge resistance increases. However, in previous studies [10] of shallowly inverted InAs/GaSb QWs, the quantized conductance plateaus are found to persist under external magnetic fields, in contrast with the theoretical expectations for TRS-protected helical edge states.

Importantly, for all devices made by strained-layer InAs/GaInSb QWs, the helical edge conductance shows clear magnetic field dependence. Specifically, for a 3 × 1.5 μm Hall bar device made by the InAs/Ga$_{0.75}$In$_{0.25}$Sb QWs, a quantized plateau of $h/2e^2$ has been observed at zero magnetic field, as shown in Figs. 4(a) and 4(b). Under a perpendicular magnetic field, as shown in Fig. 4(a), the plateau values (R_{CNP}) increase at first ($B_\perp$ below 5 T) due to TRS breaking, then decrease at higher $B_\perp$, indicating the edge states undergoing a transition from helical edge states to chiral edge states [10]. Similar behaviors were observed for the longer sample of 100 × 50 μm Hall bar, as shown in Figs. 4(c) and 4(d).

The response to an in-plane field $B_{//}$ shows an interesting behavior. Under a small $B_{//}$ up to 3 T [Fig. 4(b)], the measured resistance of the 3 × 1.5 μm Hall bar increases due to TRS breaking. For $B_{//}$ above 3 T, we observed that the sample resistance decreases with $B_{//}$, primarily because the bulk becomes conductive under higher $B_{//}$ (see Figs. S4 and S5 of Supplemental Material [29]).

The following comments are in order. (1) The helical edge states here should be described as a weakly interacting one-dimensional helical liquid without axial spin symmetry; i.e., spin S_z is momentum dependent [30,31]. Consequently, additional TRS-allowed inelastic scattering
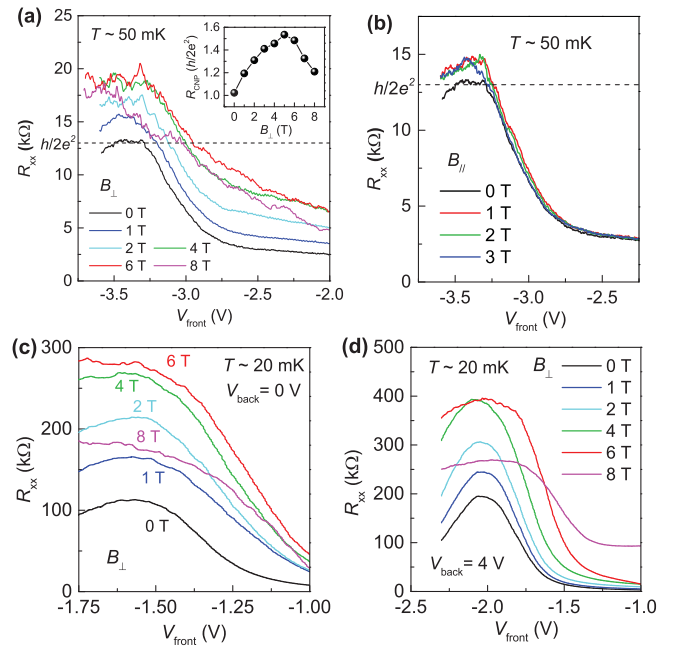

FIG. 4. Helical edge conductance under magnetic field. (a) R_{xx}-V_{front} traces of a 3×1.5 μm Hall bar under different perpendicular magnetic field ($V_{back} = 0$ V). Inset in (a): the R_{CNP} values increase monotonically in the range of $B_\perp < 5$ T, manifesting enhanced backscattering processes in the helical edge under TRS breaking. (b) R_{xx}-V_{front} traces of the 3×1.5 μm Hall bar under different in-plane magnetic fields. The plateau resistance values rise above the quantized value under $B_{//}$ because of TRS breaking. R_{xx}-V_{front} traces of the 100 $\mu m \times 50$ μm Hall bar under different perpendicular magnetic field at (c) $V_{back} = 0$ V and (d) $V_{back} = 4$ V.

channels exist. Our data show that an external magnetic field (either $B_\perp$ or $B_{//}$, or a combination of both) would cause the edge resistance R_{xx} to increase, qualitatively consistent with this spin texture picture. (2) Maciejko *et al.* [32] studied the combined effect of disorder and TRS breaking on quantum spin Hall edge transport. They conclude that in the absence of TRS, the edge liquid is topologically equivalent to a spinless one-dimensional quantum wire, and therefore subject to Anderson localization by disorder. We note that (refer to Fig. 4) under magnetic field the R_{xx} increases throughout the bulk gap, indicating that bulk disorder may play a role in localization of the edge states [32]. (3) It appears that the response of R_{xx} to a magnetic field correlates with λ_φ (hence with v_F). This can be seen in a 100 × 50 μm Hall bar under $B_\perp = 1$ T at $V_{back} = 0$ V [Fig. 4(c)] and $V_{back} = 4$ V [Fig. 4(d)], where R_{xx} increases by 41% (32%) for $\lambda_\varphi \sim 10.7$ μm (6.8 μm), respectively.

Discussion on Luttinger parameter K.—One of the most attractive features of the strained-layer InAs/GaInSb system is the relatively large hybridization gap, and the gap size can be well controlled by the strain of the QWs. A larger hybridization gap leads to an increasing edge v_F. Electron-electron interaction effects in the helical edge can

be parametrized by K, and K is strongly correlated with v_F and other factors such as screening from the environment [19,20]. In general, the helical Luttinger liquid has several fixed points in the axis of K, namely, $K = 1$, $K = 1/2$, and $K = 1/4$. For helical edge states in (regular) InAs/GaSb QWs [24] assuming $v_F \sim 5 \times 10^4$ ms^{-1}, we have determined $K \sim 0.22$, which is close to $1/4$.

As for the strained-layer InAs/GaInSb system, if we adopt a hybridization gap ~ 20 meV, n_{cross} from $(1 \text{ to } 2) \times 10^{11}$ cm^{-2}, QWs width ~ 12 nm, and screening length ~ 50 nm, the estimated v_F of helical edge states ranges then from ~ 1.9 to $\sim 1.3 \times 10^5$ ms^{-1}, and consequently the K value from ~ 0.5 to ~ 0.43. Thus, even without further refining, the present system should cover the range of $1/4$ (strongly interacting) through $1/2$ (weakly interacting) in the Luttinger parameter.

Summary.—By strain engineering, we have demonstrated for the first time a QSHI in InAs/GaInSb QWs clearly manifesting TRS protection, which shows a larger hybridization gap and longer characteristic length than existing QSHI systems. Moreover, the bulk is insulating enough at low temperatures and the edge characteristic length may be well controlled by the gates; data show that the edge states can be gapped out by applying magnetic fields. Our findings not only move one step closer to the device and circuit applications of QSHI based on semiconductor technology, but also provide a nearly ideal system for creating, detecting, and manipulating Majorana or parafermion bound states.

L. D. and T. L. contributed equally to this work.

---

*Corresponding author.
rrd@rice.edu

[1] M. Z. Hasan and C. L. Kane, Colloquium: Topological insulators, Rev. Mod. Phys. **82**, 3045 (2010).

[2] X. L. Qi and S. C. Zhang, Topological insulator and superconductors, Rev. Mod. Phys. **83**, 1057 (2011).

[3] C. L. Kane and E. J. Mele, Z_2 Topological Order and the Quantum Spin Hall Effect, Phys. Rev. Lett. **95**, 146802 (2005).

[4] B. A. Bernevig, T. L. Hughes, and S. C. Zhang, Quantum spin Hall effect and topological phase transition in HgTe quantum wells, Science **314**, 1757 (2006).

[5] M. König, S. Wiedmann, C. Brüne, A. Roth, H. Buhmann, L. W. Molenkamp, X. L. Qi, and S. C. Zhang, Quantum spin Hall insulator state in HgTe quantum wells, Science **318**, 766 (2007).

[6] M. J. Yang, C. H. Yang, B. R. Bennett, and B. V. Shanabrook, Evidence of a Hybridization Gap in "Semimetallic" InAs/GaSb Systems, Phys. Rev. Lett. **78**, 4613 (1997).

[7] C. X. Liu, T. L. Hughes, X. L. Qi, K. Wang, and S. C. Zhang, Quantum Spin Hall Effect in Inverted Type-II Semiconductors, Phys. Rev. Lett. **100**, 236601 (2008).

[8] I. Knez, R. R. Du, and G. Sullivan, Finite conductivity in mesoscopic Hall bars of inverted InAs/GaSb quantum wells, Phys. Rev. B **81**, 201301(R) (2010).

[9] I. Knez, R. R. Du, and G. Sullivan, Evidence for Helical Edge Modes in Inverted InAs/GaSb Quantum Wells, Phys. Rev. Lett. **107**, 136603 (2011).

[10] L. Du, I. Knez, G. Sullivan, and R. R. Du, Robust Helical Edge Transport in Gated InAs/GaSb Bilayers, Phys. Rev. Lett. **114**, 096802 (2015).

[11] W. Pan, J. F. Klem, J. K. Kim, M. Thalakulam, M. J. Cich, and S. K. Lyo, Chaotic quantum transport near the charge neutrality point in inverted type-II InAs/GaSb field-effect transistors, Appl. Phys. Lett. **102**, 033504 (2013).

[12] K. Suzuki, Y. Harada, K. Onomitsu, and K. Muraki, Gate-controlled semimetal-topological insulator transition in an InAs/GaSb heterostructure, Phys. Rev. B **91**, 245309 (2015).

[13] S. Mueller, A. N. Pal, M. Karalic, T. Tschirky, C. Charpentier, W. Wegscheider, K. Ensslin, and T. Ihn, Nonlocal transport via edge states in InAs/GaSb coupled quantum wells, Phys. Rev. B **92**, 081303(R) (2015).

[14] F. Qu, A. J. A. Beukman, S. Nadj-Perge, M. Wimmer, B. M. Nguyen, W. Yi, J. Thorp, M. Sokolich, A. A. Kiselev, M. J. Manfra, C. M. Marcus, and L. P. Kouwenhoven, Electric and Magnetic Tuning between the Trivial and Topological Phases in InAs/GaSb Double Quantum Wells. Phys. Rev. Lett. **115**, 036803 (2015).

[15] F. Couëdo, H. Irie, K. Suzuki, K. Onomitsu, and K. Muraki, Single-edge transport in an InAs/GaSb quantum spin Hall insulator, Phys. Rev. B **94**, 035301 (2016).

[16] F. Nichele, H. J. Suominen, M. Kjaergaard, C. M. Marcus, E. Sajadi, J. A. Folk, F. Qu, A. J. A. Beukman, and F. K. de Vries, Edge transport in the trivial phase of InAs/GaSb, New J. Phys. **18**, 083005 (2016).

[17] B. M. Nguyen, A. A. Kiselev, R. Noah, W. Yi, F. Qu, A. J. A. Beukman, F. K. de Vries, J. van Veen, S. Nadj-Perge, L. P. Kouwenhoven, M. Kjaergaard, H. J. Suominen, F. Nichele, C. M. Marcus, M. J. Manfra, and M. Sokolich, Decoupling Edge Versus Bulk Conductance in the Trivial Regime of an InAs/GaSb Double Quantum Well Using Corbino Ring Geometry, Phys. Rev. Lett. **117**, 077701 (2016).

[18] C. Wu, B. A. Bernevig, and S. C. Zhang, Helical Liquid and the Edge of Quantum Spin Hall Systems, Phys. Rev. Lett. **96**, 106401 (2006).

[19] J. C. Y. Teo and C. L. Kane, Critical behavior of a point contact in a quantum spin Hall insulator, Phys. Rev. B **79**, 235321 (2009).

[20] J. Maciejko, C. Liu, Y. Oreg, X. L. Qi, C. Wu, and S. C. Zhang, Kondo Effect in the Helical Edge Liquid of the Quantum Spin Hall State, Phys. Rev. Lett. **102**, 256803 (2009).

[21] Y. Naveh and B. Laikhtman, Excitonic Instability and Electric-Field-Induced Phase Transition Towards a Two-Dimensional Exciton Condensate, Phys. Rev. Lett. **77**, 900 (1996).

[22] D. I. Pikulin and T. Hyart, Interplay of Exciton Condensation and the Quantum Spin Hall Effect in InAs/GaSb Bilayers, Phys. Rev. Lett. **112**, 176403 (2014).

[23] L. Du, W. Lou, K. Chang, G. Sullivan, and R. R. Du, Gate-tuned spontaneous exciton insulator in double-quantum wells, arXiv:1508.04509.

[24] T. Li, P. Wang, H. Fu, L. Du, K. A. Schreiber, X. Mu, X. Liu, G. Sullivan, G. A. Csáthy, X. Lin, and R. R. Du, Observation of a Helical Luttinger Liquid in InAs/GaSb Quantum Spin Hall Edges, Phys. Rev. Lett. **115**, 136804 (2015).

[25] E. Tang and L. Fu, Strain-induced partially flat band, helical snake states and interface superconductivity in topological crystalline insulators, Nat. Phys. **10**, 964 (2014).

[26] I. Zeljkovic, D. Walkup, B. A. Assaf, K. L. Scipioni, R. Sankar, F. Chou, and V. Madhavan, Strain engineering Dirac surface states in heteroepitaxial topological crystalline insulator thin films, Nat. Nanotechnol. **10**, 849 (2015).

[27] D. L. Smith and C. Mailhiot, Proposal for strained type II superlattice infrared detectors, J. Appl. Phys. **62**, 2545 (1987).

[28] F. Fuchs, U. Weimer, W. Pletschen, J. Schmitz, E. Ahlswede, M. Walther, J. Wagner, and P. Koidl, High performance InAs/Ga$_{1-x}$In$_x$Sb superlattice infrared photodiodes, Appl. Phys. Lett. **71**, 3251 (1997).

[29] See Supplemental Material http://link.aps.org/supplemental/10.1103/PhysRevLett.119.056803 for wafer characterizations, and more data about temperature and magnetic field dependence.

[30] A. Rod, T. L. Schmidt, and S. Rachel, Spin texture of generic helical edge states, Phys. Rev. B **91**, 245112 (2015).

[31] T. L. Schmidt, S. Rachel, F. von Oppen, and L. I. Glazman, Inelastic Electron Backscattering in a Generic Helical Edge Channel, Phys. Rev. Lett. **108**, 156402 (2012).

[32] J. Maciejko, X. L. Qi, and S. C. Zhang, Magnetoconductance of the quantum spin Hall state, Phys. Rev. B **82**, 155310 (2010).